iScience

CellPress
OPEN ACCESS

Article

TC-14, a cathelicidin-derived antimicrobial peptide with broad-spectrum antibacterial activity and high safety profile

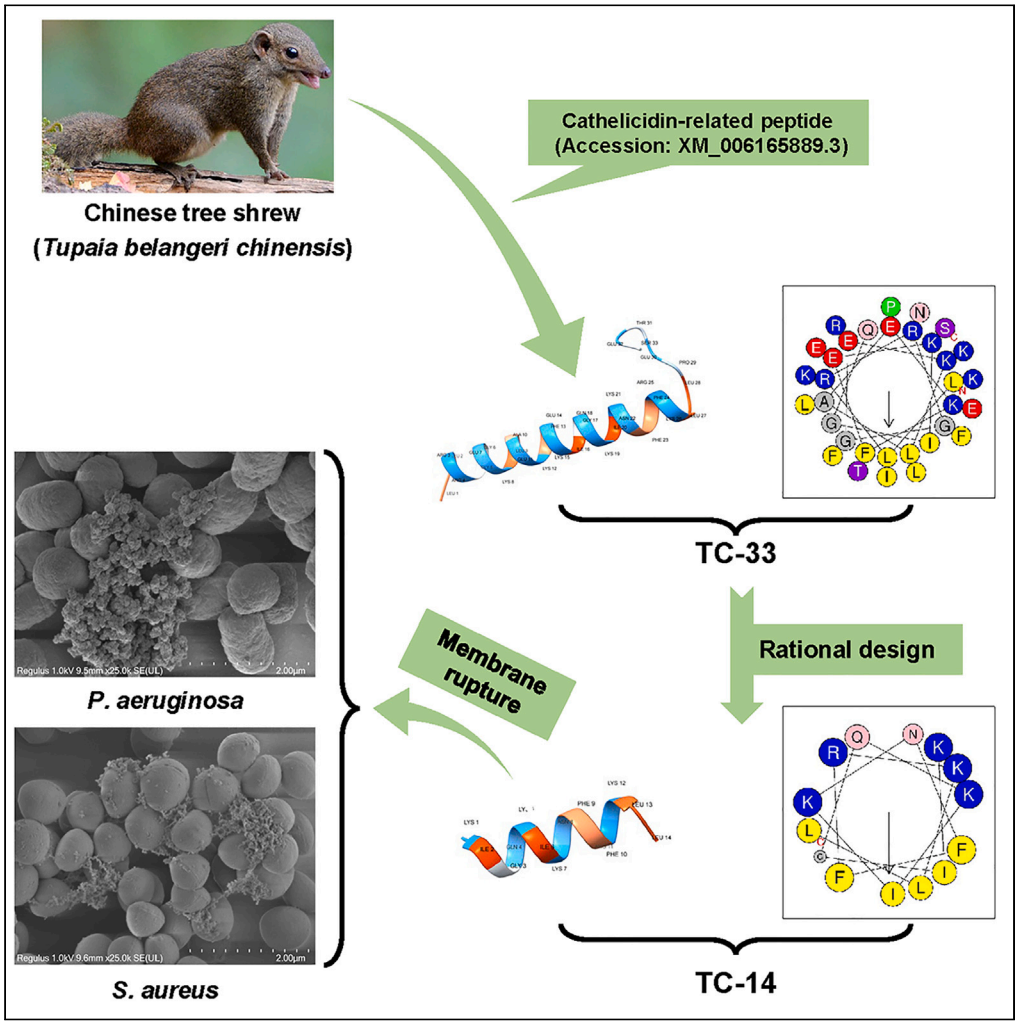

Chenxi Li, Ying Cai, Lin Luo, ..., Tianyu Zhang, Wenlin Chen, Zhiye Zhang

zty20231989@163.com (T.Z.)
chenwenlin1@hotmail.com (W.C.)
zhangzhiye5225@163.com (Z.Z.)

Highlights

A cathelicidin AMP (TC-33) was identified from the Chinese tree shrew identified

TC-14 was designed with 4–32 times higher antimicrobial activity than TC-33

TC-14 is highly biocompatible and safe *in vivo*

TC-14 was a promising drug candidate for antimicrobial drug development

Li et al., iScience *27*, 110404
July 19, 2024
https://doi.org/10.1016/j.isci.2024.110404

iScience

CellPress
OPEN ACCESS

Article

TC-14, a cathelicidin-derived antimicrobial peptide with broad-spectrum antibacterial activity and high safety profile

Chenxi Li,[1,2,5] Ying Cai,[1,5] Lin Luo,[1,2,5] Gengzhou Tian,[3,5] Xingyu Wang,[1,4] An Yan,[1] Liunan Wang,[1] Sijing Wu,[1,4] Zhongxiang Wu,[1] Tianyu Zhang,[1,*] Wenlin Chen,[2,*] and Zhiye Zhang[1,6,*]

SUMMARY

Cathelicidins, a major class of antimicrobial peptides (AMPs), hold considerable potential for antimicrobial drug development. In the present study, we identified a novel cathelicidin AMP (TC-33) derived from the Chinese tree shrew. Despite TC-33 demonstrating weak antimicrobial activity, the novel peptide TC-14, developed based on its active region, exhibited a 432-fold increase in antimicrobial activity over the parent peptide. Structural analysis revealed that TC-14 adopted an amphipathic α-helical conformation. The bactericidal mechanism of TC-14 involved targeting and disrupting the bacterial membrane, leading to rapid membrane permeabilization and rupture. Furthermore, TC-14 exhibited a high-safety profile, as evidenced by the absence of cytotoxic and hemolytic activities, as well as high biocompatibility and safety *in vivo*. Of note, its potent antimicrobial activity provided significant protection in a murine model of skin infection. Overall, this study presents TC-14 as a promising drug candidate for antimicrobial drug development.

INTRODUCTION

The introduction of antibiotics in clinical medicine has saved innumerable lives and revolutionized the treatment of previously incurable bacterial infections.[1] However, this advancement has been accompanied by the rapid emergence and spread of antibiotic-resistant bacteria, precipitating the current crisis of antimicrobial resistance.[2,3] Recent estimates suggest that antibiotic-resistant infections are responsible for an additional 1.27 million deaths annually, with projections indicating that this number could exceed 10 million by 2050.[4] This escalating resistance highlights the urgent need for the development of novel agents for the prevention and treatment of drug-resistant bacterial infections.

Given their broad-spectrum activities and reduced propensity to induce drug resistance, antimicrobial peptides (AMPs) have emerged as a promising alternative in addressing these challenges.[5,6] In nature, AMPs are highly diverse, with most AMPs described in amphibians. They are released as synergistic cocktails *in vivo*.[7–11] Unlike most antibiotics, which typically target a single primary site or mode of action, thus increasing their propensity for resistance development,[12] AMPs generally disrupt bacterial membranes. This distinct mode of action leads to the rapid destabilization and disintegration of the inner and outer bacterial membranes,[6] with both laboratory and clinical studies indicating a lower likelihood of resistance development against AMPs compared to traditional antibiotics.[13–15] AMPs also hold considerable potential for enhancing the efficacy of small-molecule antibiotics and combatting multidrug-resistant microbes.[16] Despite their promise, however, substantial challenges remain for the clinical application of AMPs, particularly regarding their stability, cytotoxicity, and bioavailability.[17,18]

Cathelicidins, a major class of AMPs, are found in all vertebrates, from hagfish to humans.[19,20] Their precursor structure includes a highly conserved signal sequence, an N-terminal cathelin domain, and an antimicrobial C-terminal domain. At present, the Antimicrobial Peptide Database contains a total of 153 unique cathelicidins.[11] Cathelicidins offer two main advantages for therapeutic drug development: they are highly cationic,[21] with an average net charge of +8.03,[11] and they primarily assume an amphipathic α-helical structure,[22] although a few cathelicidins can also form β sheet and β hairpin structures.[22–24] These characteristics are strongly associated with their antimicrobial activity. However, the relatively long primary sequences of most cathelicidins, averaging 34.38 residues,[11] lead to high production costs, susceptibility to enzymatic degradation, and potential immunogenicity. To reduce the synthesis costs and facilitate the clinical application of AMPs as

[1]Institute of Medical Biology, Chinese Academy of Medical Sciences & Peking Union Medical College, Kunming 650031, Yunnan, China
[2]Third Department of Breast Surgery, Peking University Cancer Hospital Yunnan, Third Affiliated Hospital of Kunming Medical University (Yunnan Cancer Hospital), Kunming 650118, Yunnan, China
[3]Department of Breast Surgery, First Affiliated Hospital of Kunming Medical University, Kunming, Yunnan 650032, China
[4]School of Life Sciences, Yunnan University, Kunming 650500, China
[5]These authors contributed equally
[6]Lead contact
*Correspondence: zty20231989@163.com (T.Z.), chenwenlin1@hotmail.com (W.C.), zhangzhiye5225@163.com (Z.Z.)
https://doi.org/10.1016/j.isci.2024.110404

Table 1. Physicochemical parameters of TC-33 and TC-14

Peptide	TC-33	TC-14
Sequence	LLRRGGEKLAEKFEKIGQKIKNFFRKLLPETES-NH_2	KIGQKIKNFFRKLL-NH_2
Length	33	14
Net charge	+4	+5
Hydrophobicity	0.174	0.342
Polar residues (n/%)	21/63.64	8/57.14
Nonpolar residues (n/%)	12/36.36	6/42.86

antibacterial agents, it is necessary to trim non-essential regions and identify the active domains within larger AMPs responsible for antimicrobial activity.[13,25]

The Chinese tree shrew (*Tupaia belangeri chinensis*), a small rat-sized mammal resembling a squirrel, is widely distributed across Southeast Asia and the southern and southwestern regions of China. Increasing evidence suggests that the tree shrew possesses several distinct traits, establishing it as an ideal subject for experimental research.[26] While the annotated genome of this species, released in 2013,[27] predicted the presence of a cathelicidin-related peptide (GenBank: XM_006165889.3), the intrinsic antimicrobial capabilities of this peptide remain to be determined.

In this study, the predicted cathelicidin-like peptide (TC-33) was synthesized and functionally evaluated, revealing limited antimicrobial activity. As such, a novel peptide (TC-14) derived from the active region of TC-33 was developed to enhance therapeutic effectiveness and reduce synthesis costs. Notably, TC-14 exhibited significantly improved antimicrobial activity compared to the original peptide.

RESULTS

Identification and characterization of tree shrew cathelicidin

Using the predicted precursor of the tree shrew cathelicidin, the mature peptide form consisting of 33 amino acids was identified and named TC-33 (Table 1). TC-33 exhibited a net charge of +4 at physiological pH, indicating a moderately cationic nature. Sequence-based structural predictions indicated that TC-33 could form an amphipathic structure, with hydrophilic amino acids primarily clustered on one side and hydrophobic residues clustered on the other (Figures 1A and 1B). After synthesizing TC-33 with a C-terminal amide, its antimicrobial properties were assessed against *Acinetobacter baumannii*, *Pseudomonas aeruginosa*, *Escherichia coli*, and *Staphylococcus aureus*, which pose considerable public health threats.[28] As shown in Table 2, TC-33 demonstrated weak antimicrobial activity against these bacteria, with minimal inhibitory concentrations (MICs) ranging from 37.5 to 150 μg/mL.

Identification of active region in tree shrew cathelicidin

TC-33 contained five acidic glutamate residues, reducing its cationicity and possibly contributing to its low activity.[6,14] To identify the active region within TC-33 and lower the costs of peptide synthesis, a smaller peptide was designed based on the removal of 14 amino acids from the N-terminal and five from the C-terminal of TC-33, yielding a 14-amino acid peptide termed TC-14 (Table 1). TC-14 was characterized as a cationic peptide with a net positive charge of +5. Based on its helical structure and amphiphilic nature (Figures 1C and 1D), TC-14 exhibited superior amphipathic α-helical characteristics and higher surface electrostatic potential compared to TC-33 (Figure 1).

To confirm the accuracy of the predicted structure, the secondary structures of TC-33 and TC-14 were determined in sodium dodecyl sulfate (SDS) micelles, simulating a membrane environment, using circular dichroism (CD) spectroscopy. The CD spectra and spectral analysis of TC-14 and its parent peptide (Figure 2) demonstrated a predominantly unstructured form in aqueous solution, as evidenced by low ellipticity above 210 nm and a minimum near 198 nm.[29,30] Conversely, in the presence of SDS (8 or 64 mM), they primarily formed an α-helical structure, characterized by dual negative bands at 208 and 222 nm and a positive band at 195 nm.[29,30] Specially, the α-helical content of TC-14 was higher than that of its parent peptide TC-33 in the presence of SDS (Figures 2C and 2D), suggesting it may permeabilize bacterial membranes more efficiently.

The antimicrobial efficacy of TC-14 was subsequently determined. Notably, TC-14 displayed improved antimicrobial activities compared to TC-33, with MICs ranging from 2.34 to 9.38 μg/mL (Table 2), demonstrating a 432-fold increase in activity relative to its parent peptide. Furthermore, the antimicrobial activity of TC-14 was tested against clinical isolates of *A. baumannii*, *P. aeruginosa*, *E. coli*, and methicillin-resistant *S. aureus* (MRSA). Remarkably, TC-14 exerted potent antibacterial activities, with MIC values of 1.17–2.34 μg/mL against *A. baumannii*, 4.69–18.75 μg/mL against *P. aeruginosa*, 4.69–9.38 μg/mL against *E. coli*, and 1.17–4.69 μg/mL against MRSA (Table S1). These findings suggest that TC-14 represents the active region of TC-33.

TC-33 and TC-14 show no hemolytic or cytotoxic activity

The development of AMP-based therapies is hindered by their hemolytic and cytotoxic effects.[31–33] Here, assessment revealed that neither TC-33 nor TC-14 displayed cytotoxic (Figures 3A and 3C) or hemolytic activity (Figures 3B and 3D), even at concentrations as high as 100 μg/mL. Thus, given its favorable safety profile and potent activity, our subsequent studies focused predominantly on TC-14.

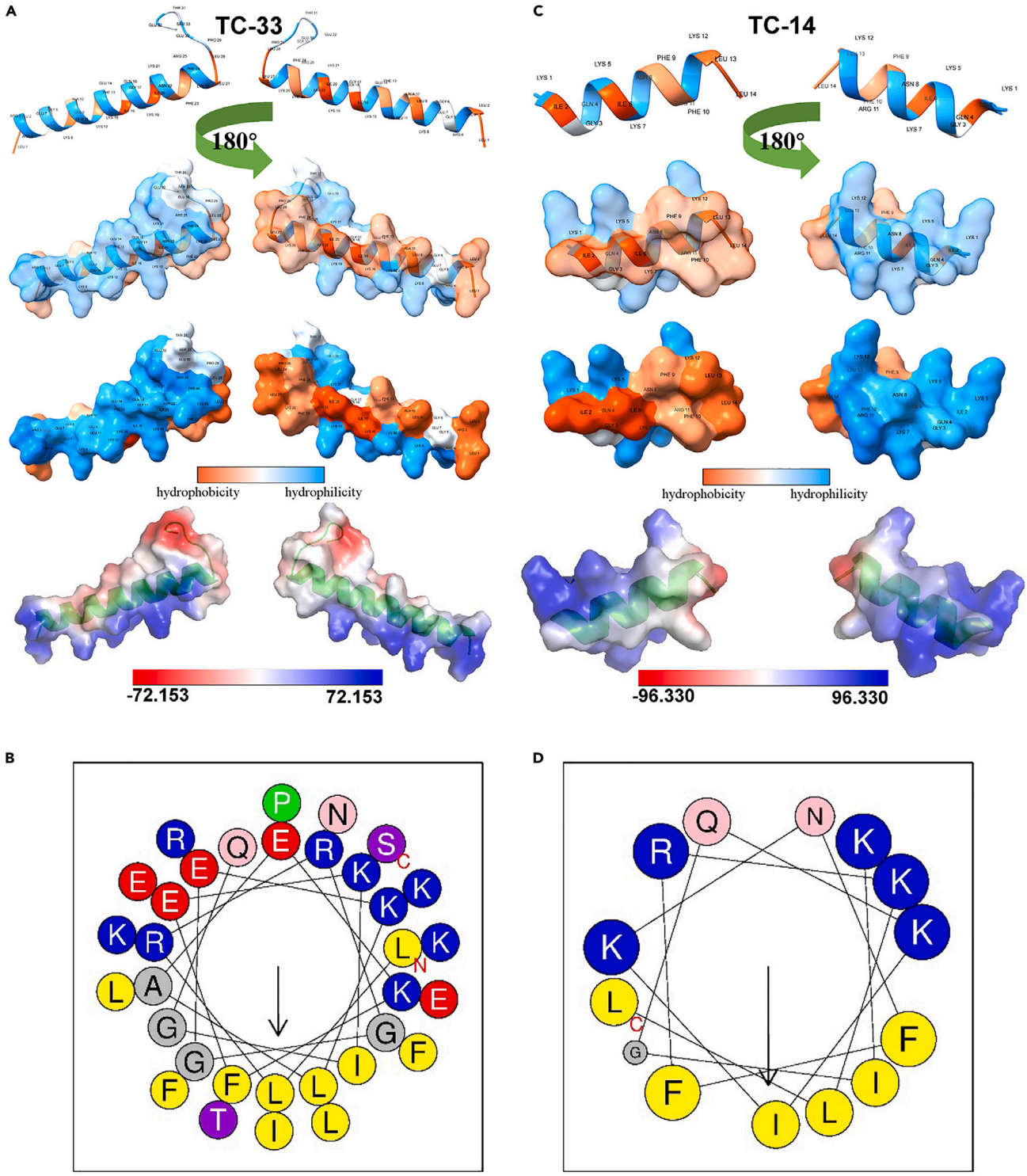

Figure 1. Three-dimensional characterization and helical wheel projections of TC-33 and TC-14

(A and C) *De novo* structural predictions and amphiphilicity analysis of TC-33 (A) and TC-14 (C), with blue representing hydrophilicity and orange representing hydrophobicity. Surface electrostatic potential was analyzed using PyMOL, with blue representing positive charge and red representing negative charge. (B and D) Helical wheel projections of TC-33 (B) and TC-14 (D). Hydrophobic residues are shown in yellow, positively charged hydrophilic residues are shown in blue, uncharged polar residues are shown in purple, and negatively charged hydrophilic residues are shown in red.

Table 2. Antimicrobial activities of TC-14 and its analogs

	MIC (μg/mL)				
Bacterial strain	TC-33	TC-14	Colistin	Ampicillin	Vancomycin
E. coli ATCC8739	150	9.38	0.59	–	–
A. baumannii ATCC19606	75	2.34	0.59	–	–
P. aeruginosa ATCC27853	37.5	9.38	4.69	–	–
S. aureus ATCC6538	75	4.69	–	9.38	1.17

These MICs represent mean values of three independent experiments. See also Table S1.

TC-14 kills bacteria by inducing membrane permeabilization and rupture

To elucidate the potential mechanism of action of TC-14, its impact on bacterial membrane permeation was examined using fluorescence assay. Propidium iodide (PI), a small fluorescent molecule that intensifies in fluorescence upon binding to DNA or RNA, cannot penetrate intact cellular membranes. The addition of TC-14 to gram negative *E. coli* (Figure 4A), *A. baumannii* (Figure 4B), and *P. aeruginosa* (Figure 4C) resulted in an immediate and time-dependent increase in PI influx, suggesting changes in the permeability of the bacterial membrane. Colistin, known for disrupting bacterial membranes, also exhibited an immediate effect on PI influx. Similarly, the application of TC-14 to *S. aureus* (Figure 4D) induced a rapid increase in PI influx. In contrast, vancomycin, an inhibitor of peptidoglycan synthesis in gram positive bacteria, showed no effect on PI influx. These findings suggest that TC-14 can rapidly permeabilize bacterial membranes.

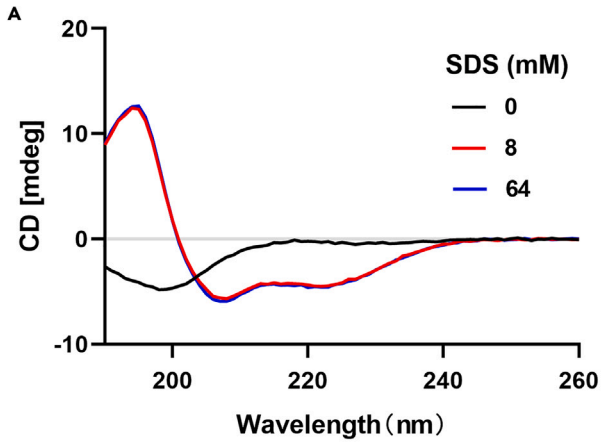

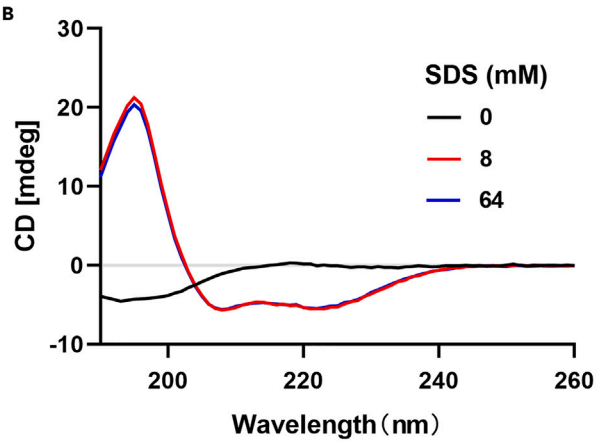

C

Structure fractions	SDS (mM)		
	0	8	64
α-Helix content (%)	9.5	58	57.43
β-sheet content (%)	28.79	15	18.81
γ-turn content (%)	24.39	11	7.92
Random coil (%)	37.33	16	15.84

D

Structure fractions	SDS (mM)		
	0	8	64
α-Helix content (%)	8.85	69.7	74
β-sheet content (%)	27.7	18.18	14
γ-turn content (%)	24.2	6.06	3
Random coil (%)	39.25	6.06	9

Figure 2. CD spectra of TC-33 and TC-14

CD spectra of TC-33 (A) and TC-14 (B) (200 μg/mL) in different concentrations of SDS (0, 8, and 64 mM). Graph depicts representative measurements of three independent replicates. TC-33 (C) and TC-14 (D) Further CD spectral analysis was carried out to predict secondary structure characteristics using the deconvolution program DichroWeb (http://dichroweb.cryst.bbk.ac.uk/html/home.shtml). See also Figure S2.

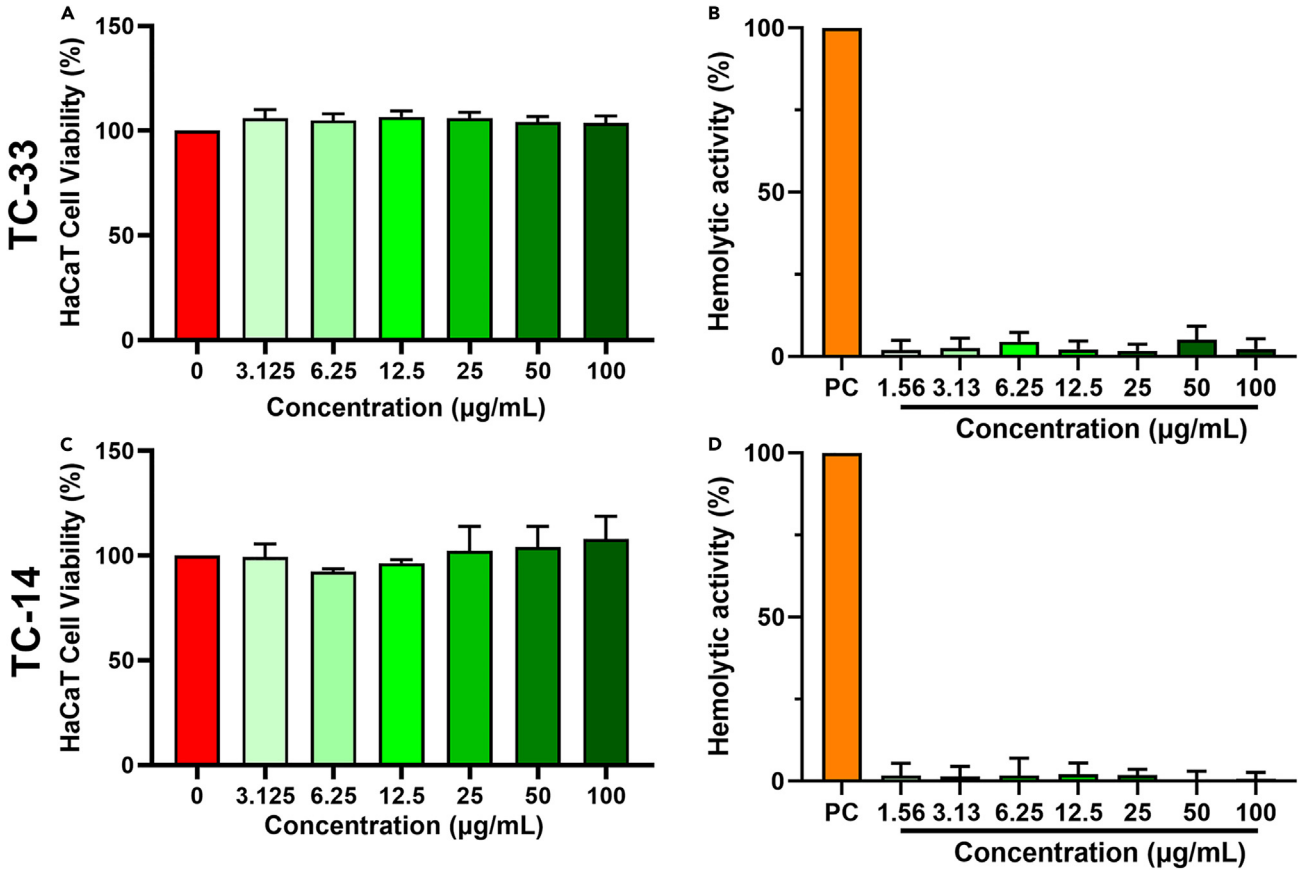

Figure 3. Cytotoxicity and hemolytic activity of TC-33 and TC-14

Potential toxicity of TC-33 (A) and TC-14 (C) on human HaCaT keratinocytes. Potential hemolysis of TC-33 (B) and TC-14 (D) on human erythrocytes. Sterile saline and 1% (v/v) Triton X-100 were used as negative (NC) and positive (PC) controls, respectively. Data represent mean ± SD of three independent experiments.

The morphological changes in *P. aeruginosa* and *S. aureus* cells after TC-14 treatment were further explored using SEM and transmission electron microscopy (TEM). As illustrated in Figure 5A, normal saline-treated (vehicle) *P. aeruginosa* cells appeared as rods with bright and smooth surfaces. In contrast, significant structural changes, including membrane disruption, cellular content leakage, and cytoplasmic clear zones were observed in the TC-14-treated bacteria. Exposure to colistin resulted in noticeable membrane roughening and corrugation, without evident cellular leakage. Similarly, TC-14 treatment of *S. aureus* led to significant structural alterations, including cell membrane disruption with visible pore formation and bacterial inclusion leakage (Figure 5B). Conversely, vancomycin treatment resulted in limited cell lysis in *S. aureus*, with most cells appearing normal. Overall, these results indicate that TC-14 can effectively permeabilize and disrupt microbial membranes.

TC-14 shows medium killing rate and low propensity to induce resistance

To assess the bactericidal properties of TC-14, kinetic analyses were carried out with *A. baumannii* and *S. aureus*. As shown in Figures 6A and 6B, results indicated that the bactericidal activity of TC-14 increased with prolonged exposure, leading to a reduction in colony-forming unit (CFU) counts. Specifically, TC-14 eradicated *A. baumannii* within 180 min at 5 × MIC (Figure 6A). This pattern was mirrored with colistin, which also completely eliminated *A. baumannii* within the same duration at a similar concentration. In the case of *S. aureus*, TC-14 demonstrated a time-dependent lethal effect, eradicating more than 99% of bacterial cells within 180 min at 5 × MIC, although a small number of bacteria persisted (Figure 6B). In contrast, vancomycin exhibited reduced efficacy against *S. aureus*, likely attributable to its inhibition of cell wall synthesis rather than direct killing ability within the 180 min time frame.

The emergence of resistance poses a significant global health challenge, impeding drug development and the elimination of nosocomial pathogens. As such, we evaluated resistance development by serially passaging *P. aeruginosa* and *S. aureus* up to 60 times in the presence of subinhibitory concentrations of TC-14 or control treatments. As shown in Figure 6C, serial passaging of *P. aeruginosa* with TC-14 did not result in the development of resistant isolates, whereas colistin exposure resulted in a 2-fold increase in MIC after 35 passages. Interestingly, exposure of *S. aureus* to TC-14 led to a 2-fold increase in MIC after five passages (Figure 6D), while vancomycin exposure led to a 4-fold increase in MIC after 25 passages.

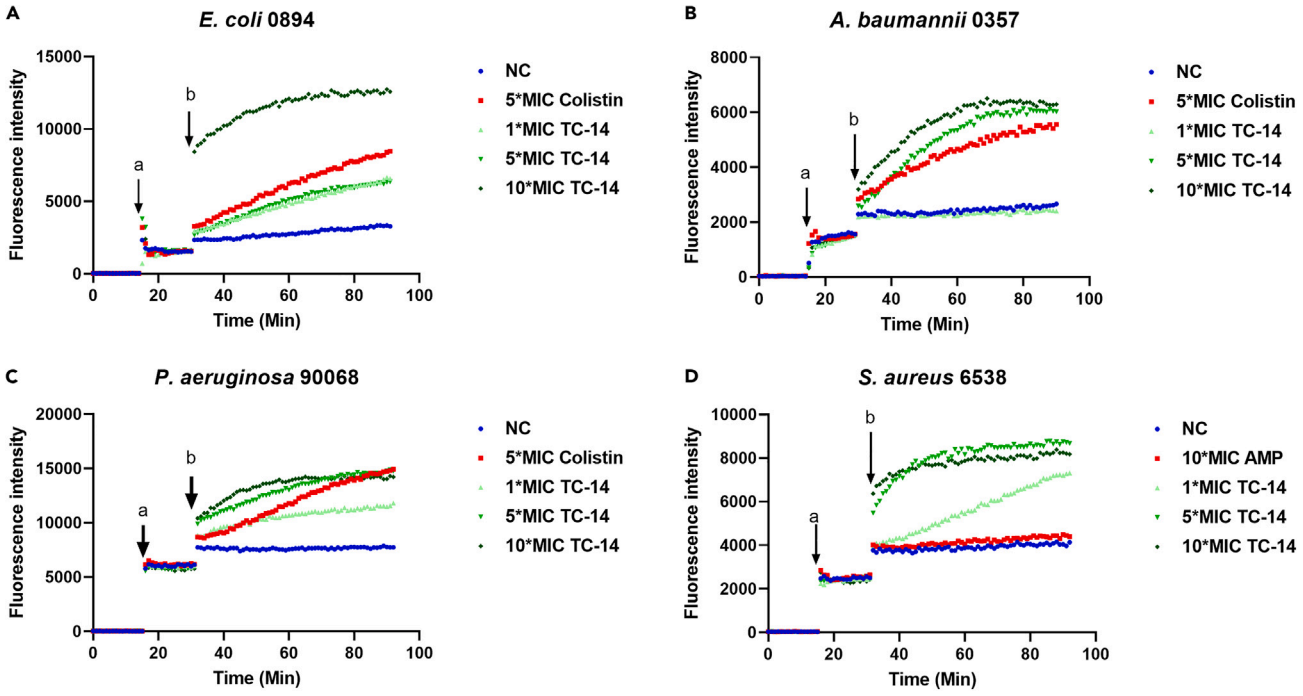

Figure 4. TC-14 induces bacterial membrane permeabilization

(A–D) *E. coli* (0894) (A), *A. baumannii* (0357) (B), *P. aeruginosa* (90068) (C), and *S. aureus* (6538) (D) were first incubated with PI for 15 min, after which the test samples were added (TC-14, 1–10 × MIC; 5 × MIC for colistin and vancomycin). Fluorescence intensities of PI were measured continuously for 90 min. Arrows indicate addition of PI (a) and test samples (b). Representative measurements of three independent replicates are depicted.

TC-14 shows therapeutic potential against skin infection

The therapeutic potential of TC-14 was subsequently assessed using a mouse skin wound infection model. Prior to the *in vivo* experiments, the effects of plasma on the antibacterial activity of TC-14 were examined. As shown in Table S2, 8-h pre-treatment with mouse plasma slightly reduced the antimicrobial activity of TC-14, resulting in a 4- to 8-fold increase in the MICs against *A. baumannii* and *S. aureus*. However, the peptide largely maintained its antibacterial activity. Furthermore, intravenous administration of TC-14 at a dose of 10 mg/kg showed no observable toxicity over a 48-h period, indicating high biocompatibility and safety of the peptide *in vivo*. In contrast, a 10 mg/kg dose of colistin proved lethal to all mice within 10 min (Figure S1).

The *in vivo* therapeutic potency of TC-14 was further evaluated using a mouse skin wound model infected with either *S. aureus* or *A. baumannii* (Figure 7A). Notably, treatment with TC-14 resulted in a dose-dependent decrease in *S. aureus* colonization, with peptide concentrations of 0.5 and 2 mg/mL significantly reducing *S. aureus* CFU counts by 57.9% and 93.1%, respectively (Figure 7B). A similar dose-dependent decline in bacterial load was observed for *A. baumannii* (Figure 7C). Vancomycin and colistin also effectively lowered bacterial counts, potentially due to their markedly lower MICs compared to TC-14 (Table 2). Collectively, these findings highlight the significant therapeutic potential of topical TC-14 for the treatment of skin infections.

DISCUSSION

AMPs represent a promising class of therapeutic agents with potent effects against bacteria, fungi, and viruses. However, many natural AMPs require further characterization and optimization for clinical use, particularly in regard to their safety, stability, and activity. One common strategy is to employ natural AMPs as models, either by truncating them or identifying their active domains, to achieve similar or superior antibacterial activity and selectivity.[13,34] For instance, the truncated derivative of dermaseptin shows improved antimicrobial properties compared to its parent peptide.[35] Studies on cathelicidins have also shown that shorter peptides can retain antibacterial activity.[25,36–39] Humans possess a single cathelicidin, whose mature form (LL-37) has been extensively studied.[40] Although LL-37 exhibits broad-spectrum activity, its efficacy against bacteria, fungi, and viruses is relatively limited.[41] Both structure-based design and library screening methods have been used to identify the active regions of LL-37, revealing a core peptide of just 13 amino acids.[25,42] In this study, we identified a novel cathelicidin AMP (TC-33) from the Chinese tree shrew. Similar to human LL-37, TC-33 exhibited weak activity (Table 2). Crucially, we identified and synthesized a novel 14-residue peptide (TC-14), which displayed markedly higher activity than the parent peptide (Tables 2 and S1). This smaller peptide likely represents the active region of TC-33, thus enabling a substantial reduction in synthesis costs while enhancing therapeutic potential.

Although TC-33 contained nine basic amino acids, its positive charges were largely neutralized by five glutamate residues, resulting in a net charge of +4, which likely contributed to its low antimicrobial activity (Table 2). To improve the antimicrobial potential of TC-33, the

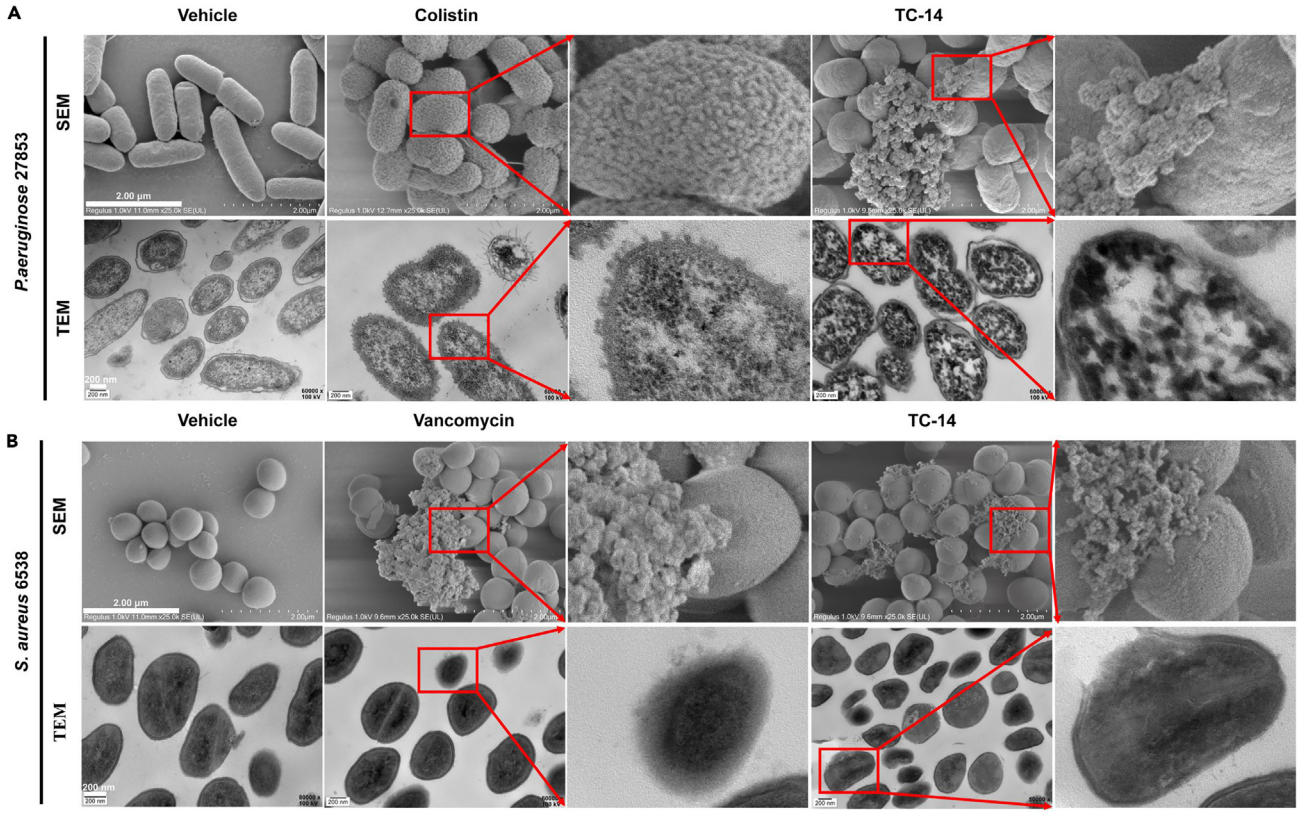

Figure 5. TC-14 induces cell membrane rupture

(A and B) SEM and TEM images showing morphological changes in *P. aeruginosa* (27853) (A) and *S. aureus* (6538) (B) treated with TC-14 (5 × MIC) or controls (colistin or vancomycin at 5 × MIC). Images are representative of three independent replicates.

glutamate-rich sequences were removed to increase its cationic nature. Additionally, the proline residue, known to prevent helix formation,[43] was eliminated, resulting in a novel 14-amino acid sequence (TC-14). Notably, TC-14 contained an additional net positive charge (+5) and exhibited greater hydrophobicity (Table 1), improved amphipathic α-helical characteristics and higher surface electrostatic potential compared to TC-33 (Figure 1), likely contributing to its enhanced antimicrobial activities. As expected, TC-14 exhibited substantially higher antimicrobial activity than TC-33 (Table 2). While higher antimicrobial activity can correlate with increased toxicity, TC-14 demonstrated no cytotoxic (Figure 3C) or hemolytic activity (Figure 3D), indicating high therapeutic potential.

AMPs are highly susceptible to degradation by proteases, which are commonly present at wound sites. These proteases can be secreted by both host skin tissues and bacteria.[44] In the present study, a mouse skin wound infection model was utilized to assess the therapeutic efficacy of TC-14. Although TC-14 significantly reduced bacterial counts in the mouse skin wounds, its activity was lower than that of vancomycin and colistin (Figure 7). This reduced efficacy could be attributed to two factors. Firstly, vancomycin and colistin exhibited MIC values 4-fold lower than that of TC-14 (Table 2), indicating 4-fold greater activity. Secondly, the activity of TC-14 may have been compromised in the presence of wound proteases, as evidenced by the reduced antimicrobial effectiveness of TC-14 following plasma treatment (Table S2).

As crucial components of the innate immune system, AMPs serve as the first line of defense against invasive pathogens. Their mechanisms of action not only include direct bacterial destruction via interactions with bacterial membranes but also the regulation of various immunomodulatory activities to enhance the host's response to infection.[45,46] Despite its limited activity against bacteria, the human LL-37 peptide exerts potent immunomodulatory effects.[47] Similarly, although we identified the active region of TC-33, its low antimicrobial activity suggests it may function as a multifaceted peptide within the innate immune system of the Chinese tree shrew.

In conclusion, this study identified a novel cathelicidin peptide from the Chinese tree shrew with relatively low antimicrobial activity. To enhance its therapeutic potential and reduce synthesis costs, the active region of this peptide was determined. The resultant peptide (TC-14) demonstrated potent and broad-spectrum bactericidal activities, with a favorable safety profile and robust effects on skin wound infections.

Limitations of the study

Due to the small sample size of the bacterial strains, there may be a selection bias. A larger group would be needed to confirm the aforementioned results.

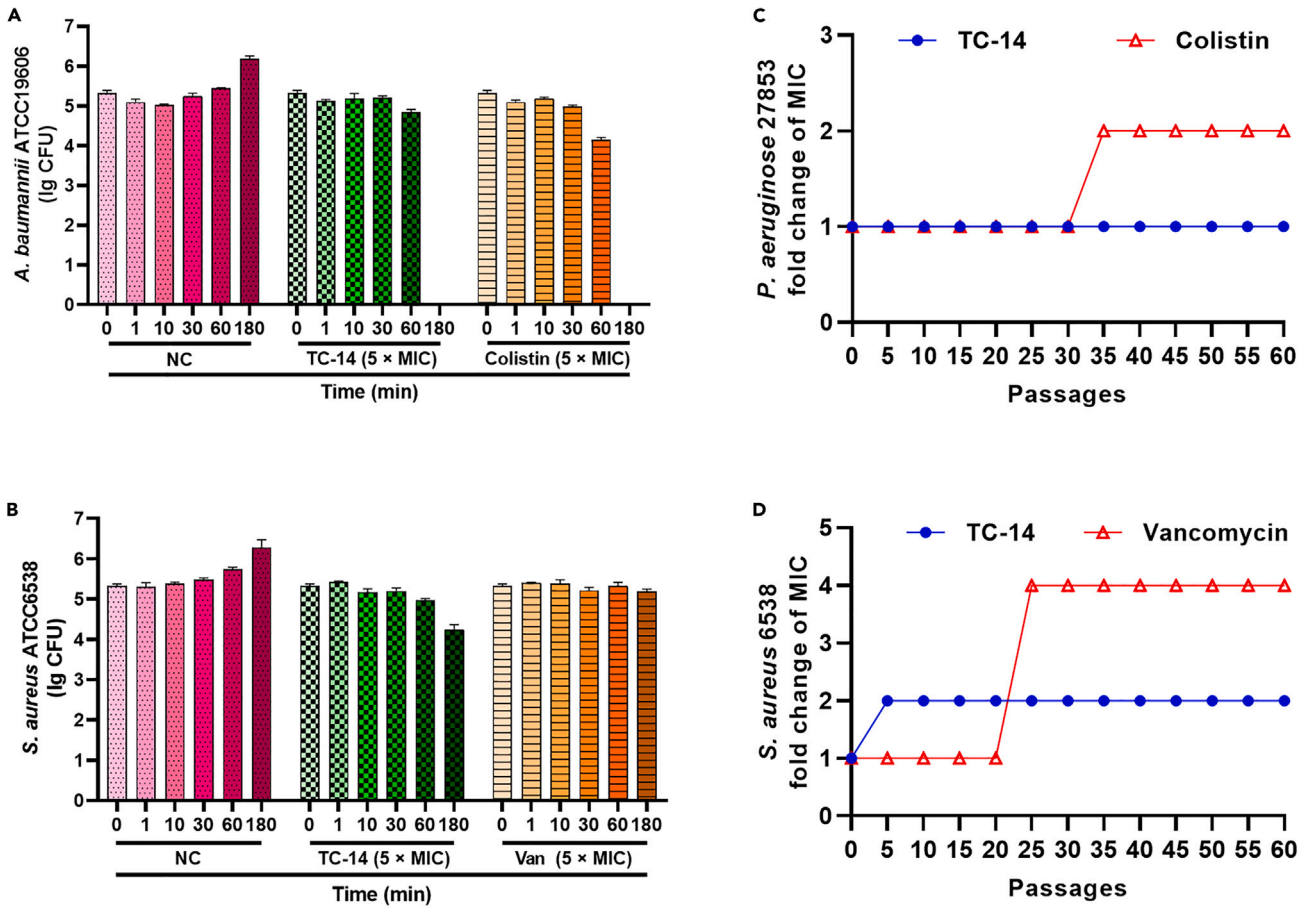

Figure 6. Bactericidal kinetics and resistance monitoring

(A–D) Bactericidal kinetics of TC-14 against *A. baumannii* (19606) (A) and *S. aureus* (6538) (B). CFU: colony forming unit; NC: saline. TC-14, colistin, and vancomycin concentrations were all 5-fold MIC. TC-14 resistance assay for *P. aeruginosa* (27853) (C) and *S. aureus* (6538) (D) induced by 60 generations. Same induction was used for colistin and vancomycin in the control group. Data represent mean ± SD of three independent experiments.

STAR★METHODS

Detailed methods are provided in the online version of this paper and include the following:

- KEY RESOURCES TABLE
- RESOURCE AVAILABILITY
  - Lead contact
  - Materials availability
  - Data and code availability
- EXPERIMENTAL MODEL AND STUDY PARTICIPANT DETAILS
  - Mouse model
- METHOD DETAILS
  - Peptide synthesis
  - Bioinformatic analysis and structural modeling
  - Circular dichroism (CD) spectroscopy
  - Antibacterial properties *in vitro*
  - Cytotoxicity assay
  - Hemolytic activity assay
  - Effects of plasma on TC-14 antibacterial activity
  - Bacterial membrane permeabilization assay
  - Scanning electron microscopy (SEM)
  - Transmission electron microscopy (TEM)

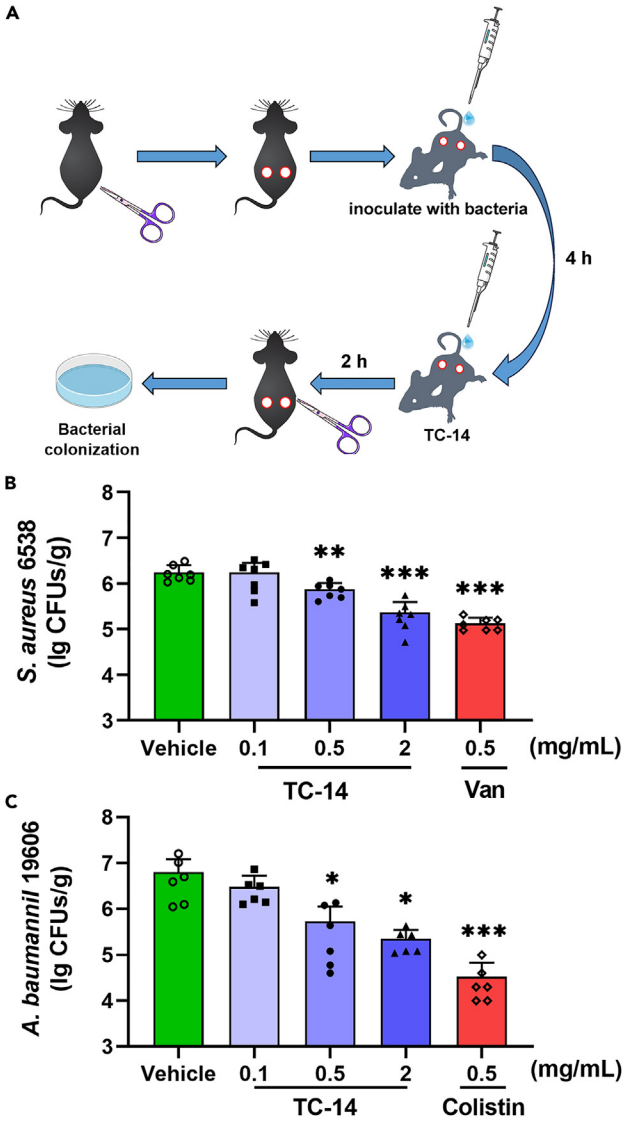

Figure 7. TC-14 protects mice against skin infection

(A) Schematic of mouse experiment. Female BALB/c mice were initially infected with *S. aureus* (6538) ($n = 7$) (B) and *A. baumannii* (19606) ($n = 6$) (C) through skin wounds. At 4 h after bacterial inoculation, 20 μL of TC-14 (0.1, 0.5, and 2 mg/mL) or control (saline as vehicle control, vancomycin or colistin (0.5 mg/mL) as positive controls) was administered. Bacterial colonization was quantified 2 h after sample application. $^{*}p < 0.05$, $^{**}p < 0.01$, $^{***}p < 0.001$, one-way ANOVA with Dunnett *post hoc* test compared with vehicle group. See also Figure S1.

- Bacteria killing kinetics
- Drug-resistant assays
- Acute toxicity analysis
- Effects of TC-14 on mouse skin wound infections

- QUANTIFICATION AND STATISTICAL ANALYSIS

SUPPLEMENTAL INFORMATION

Supplemental information can be found online at https://doi.org/10.1016/j.isci.2024.110404.

ACKNOWLEDGMENTS

This work was supported by the National Natural Science Foundation of China (32070443), Yunnan Province Grants (202302AA310015 and 202301AU070045), Fundamental Research Funds for the Central Universities (3332023081), Middle-aged and Young Academic and Technical

Leader Reserve Talent Program of Yunnan Province Science and Technology Department (202205AC160008), and Yunnan Province's Xing Dian Talent Support Program-Specialization in Medical and Health Talents.

AUTHOR CONTRIBUTIONS

Z.Z., W.C., and T.Z. conceived and supervised the project; C.L., Y.C., L.L., and G.T. performed experiments and analyzed data; X.W., A.Y., L.W., S.W., and Z.W. participated in the data analyses and revised the manuscript. Z.Z. and T.Z. wrote the paper. All the authors contributed to the discussions.

DECLARATION OF INTERESTS

The authors declare no competing interests.

Received: March 27, 2024
Revised: May 27, 2024
Accepted: June 26, 2024
Published: June 28, 2024

REFERENCES

1. Hutchings, M.I., Truman, A.W., and Wilkinson, B. (2019). Antibiotics: past, present and future. Curr. Opin. Microbiol. *51*, 72–80. https://doi.org/10.1016/j.mib.2019.10.008.
2. Jampani, M., and Chandy, S.J. (2021). Increased antimicrobial use during COVID-19: The risk of advancing the threat of antimicrobial resistance. Health Sci. Rep. *4*, e459. https://doi.org/10.1002/hsr2.459.
3. Lupo, A., Coyne, S., and Berendonk, T.U. (2012). Origin and evolution of antibiotic resistance: the common mechanisms of emergence and spread in water bodies. Front. Microbiol. *3*, 18. https://doi.org/10.3389/fmicb.2012.00018.
4. Antimicrobial Resistance Collaborators (2022). Global burden of bacterial antimicrobial resistance in 2019: a systematic analysis.
5. Xuan, J., Feng, W., Wang, J., Wang, R., Zhang, B., Bo, L., Chen, Z.S., Yang, H., and Sun, L. (2023). Antimicrobial peptides for combating drug-resistant bacterial infections. Drug Resist. Updat. *68*, 100954. https://doi.org/10.1016/j.drup.2023.100954.
6. Mwangi, J., Hao, X., Lai, R., and Zhang, Z.Y. (2019). Antimicrobial peptides: new hope in the war against multidrug resistance. Zool. Res. *40*, 488–505. https://doi.org/10.24272/j.issn.2095-8137.2019.062.
7. Tan, Y., Chen, X., Ma, C., Xi, X., Wang, L., Zhou, M., Burrows, J.F., Kwok, H.F., and Chen, T. (2018). Biological Activities of Cationicity-Enhanced and Hydrophobicity-Optimized Analogues of an Antimicrobial Peptide, Dermaseptin-PS3, from the Skin Secretion of Phyllomedusa sauvagii. Toxins *10*, 320. https://doi.org/10.3390/toxins10080320.
8. Zhou, X., Liu, Y., Gao, Y., Wang, Y., Xia, Q., Zhong, R., Ma, C., Zhou, M., Xi, X., Shaw, C., et al. (2020). Enhanced Antimicrobial Activity of N-Terminal Derivatives of a Novel Brevinin-1 Peptide from The Skin Secretion of Odorrana schmackeri. Toxins *12*, 484. https://doi.org/10.3390/toxins12080484.
9. Qin, H., Zuo, W., Ge, L., Siu, S.W.I., Wang, L., Chen, X., Ma, C., Chen, T., Zhou, M., Cao, Z., and Kwok, H.F. (2023). Discovery and analysis of a novel antimicrobial peptide B1AW from the skin secretion of Amolops wuyiensis and improving the membrane-binding affinity through the construction of the lysine-introduced analogue. Comput. Struct. Biotechnol. J. *21*, 2960–2972. https://doi.org/10.1016/j.csbj.2023.05.006.
10. Lazzaro, B.P., Zasloff, M., and Rolff, J. (2020). Antimicrobial peptides: Application informed by evolution. Science *368*, eaau5480. https://doi.org/10.1126/science.aau5480.
11. Wang, G., Li, X., and Wang, Z. (2016). APD3: the antimicrobial peptide database as a tool for research and education. Nucleic Acids Res. *44*, D1087–D1093. https://doi.org/10.1093/nar/gkv1278.
12. Brazas, M.D., and Hancock, R.E.W. (2005). Using microarray gene signatures to elucidate mechanisms of antibiotic action and resistance. Drug Discov. Today *10*, 1245–1252. https://doi.org/10.1016/S1359-6446(05)03566-X.
13. Han, Y., Zhang, M., Lai, R., and Zhang, Z. (2021). Chemical modifications to increase the therapeutic potential of antimicrobial peptides. Peptides *146*, 170666. https://doi.org/10.1016/j.peptides.2021.170666.
14. Mwangi, J., Yin, Y., Wang, G., Yang, M., Li, Y., Zhang, Z., and Lai, R. (2019). The antimicrobial peptide ZY4 combats multidrug-resistant Pseudomonas aeruginosa and Acinetobacter baumannii infection. Proc. Natl. Acad. Sci. USA *116*, 26516–26522. https://doi.org/10.1073/pnas.1909585117.
15. Deslouches, B., and Di, Y.P. (2017). Antimicrobial Peptides: A Potential Therapeutic Option for Surgical Site Infections. Clin. Surg. *2*, 1740.
16. Wang, C., Hong, T., Cui, P., Wang, J., and Xia, J. (2021). Antimicrobial peptides towards clinical application: Delivery and formulation. Adv. Drug Deliv. Rev. *175*, 113818. https://doi.org/10.1016/j.addr.2021.05.028.
17. Wang, C., Liu, X., Chen, S., Hu, F., Sun, J., and Yuan, H. (2018). Facile preparation of phospholipid-amorphous calcium carbonate hybrid nanoparticles: toward controllable burst drug release and enhanced tumor penetration. Chem. Commun. *54*, 13080–13083. https://doi.org/10.1039/c8cc07694d.
18. Domhan, C., Uhl, P., Meinhardt, A., Zimmermann, S., Kleist, C., Lindner, T., Leotta, K., Mier, W., and Wink, M. (2018). A novel tool against multiresistant bacterial pathogens: lipopeptide modification of the natural antimicrobial peptide ranalexin for enhanced antimicrobial activity and improved pharmacokinetics. Int. J. Antimicrob. Agents *52*, 52–62. https://doi.org/10.1016/j.ijantimicag.2018.03.023.
19. Uzzell, T., Stolzenberg, E.D., Shinnar, A.E., and Zasloff, M. (2003). Hagfish intestinal antimicrobial peptides are ancient cathelicidins. Peptides *24*, 1655–1667. https://doi.org/10.1016/j.peptides.2003.08.024.
20. Zasloff, M. (2002). Antimicrobial peptides in health and disease. N. Engl. J. Med. *347*, 1199–1200. https://doi.org/10.1056/NEJMe020106.
21. Tossi, A., Sandri, L., and Giangaspero, A. (2000). Amphipathic, alpha-helical antimicrobial peptides. Biopolymers *55*, 4–30. https://doi.org/10.1002/1097-0282(2000)55:1<4::AID-BIP30>3.0.CO;2-M.
22. Gennaro, R., and Zanetti, M. (2000). Structural features and biological activities of the cathelicidin-derived antimicrobial peptides. Biopolymers *55*, 31–49. https://doi.org/10.1002/1097-0282(2000)55:1<31::Aid-bip40>3.0.Co;2-9.
23. Mohanram, H., and Bhattacharjya, S. (2014). Cysteine deleted protegrin-1 (CDP-1): anti-bacterial activity, outer-membrane disruption and selectivity. Biochim. Biophys. Acta *1840*, 3006–3016. https://doi.org/10.1016/j.bbagen.2014.06.018.
24. Bhattacharjya, S., Zhang, Z., and Ramamoorthy, A. (2024). LL-37: Structures, Antimicrobial Activity, and Influence on Amyloid-Related Diseases. Biomolecules *14*, 320. https://doi.org/10.3390/biom14030320.
25. Wang, G., Narayana, J.L., Mishra, B., Zhang, Y., Wang, F., Wang, C., Zarena, D., Lushnikova, T., and Wang, X. (2019). Design of Antimicrobial Peptides: Progress Made with Human Cathelicidin LL-37. Adv. Exp. Med. Biol. *1117*, 215–240. https://doi.org/10.1007/978-981-13-3588-4_12.
26. Yao, Y.G. (2017). Creating animal models, why not use the Chinese tree shrew (Tupaia belangeri chinensis)? Zool. Res. *38*, 118–126. https://doi.org/10.24272/j.issn.2095-8137.2017.032.
27. Fan, Y., Huang, Z.Y., Cao, C.C., Chen, C.S., Chen, Y.X., Fan, D.D., He, J., Hou, H.L., Hu, L., Hu, X.T., et al. (2013). Genome of the Chinese tree shrew. Nat. Commun. *4*, 1426. https://doi.org/10.1038/ncomms2416.

28. Prioritization of Pathogens to Guide Discovery. Research and Development of New Antibiotics for Drug-Resistant Bacterial Infections, Including Tuberculosis (2017 (World Health Organization)). 1–87.
29. Miles, A.J., Janes, R.W., and Wallace, B.A. (2021). Tools and methods for circular dichroism spectroscopy of proteins: a tutorial review. Chem. Soc. Rev. *50*, 8400–8413. https://doi.org/10.1039/d0cs00558d.
30. Krishnamoorthy, R., Adhikari, P., and Anaikutti, P. (2023). Design, synthesis, and characterization of non-hemolytic antimicrobial peptides related to human cathelicidin LL-37. RSC Adv. *13*, 15594–15605. https://doi.org/10.1039/d3ra02473c.
31. Kang, Z., Wang, C., Zhang, Z., Liu, Q., Zheng, Y., Zhao, Y., Pan, Z., Li, Q., Shi, L., and Liu, Y. (2022). Spatial Distribution Control of Antimicrobial Peptides through a Novel Polymeric Carrier for Safe and Efficient Cancer Treatment. Adv. Mater. *34*, e2201945. https://doi.org/10.1002/adma.202201945.
32. Zhang, Q.Y., Yan, Z.B., Meng, Y.M., Hong, X.Y., Shao, G., Ma, J.J., Cheng, X.R., Liu, J., Kang, J., and Fu, C.Y. (2021). Antimicrobial peptides: mechanism of action, activity and clinical potential. Mil. Med. Res. *8*, 48. https://doi.org/10.1186/s40779-021-00343-2.
33. Kokel, A., and Torok, M. (2018). Recent Advances in the Development of Antimicrobial Peptides (AMPs): Attempts for Sustainable Medicine? Curr. Med. Chem. *25*, 2503–2519. https://doi.org/10.2174/0929867325666180117142142.
34. Jiang, Y., Chen, Y., Song, Z., Tan, Z., and Cheng, J. (2021). Recent advances in design of antimicrobial peptides and polypeptides toward clinical translation. Adv. Drug Deliv. Rev. *170*, 261–280. https://doi.org/10.1016/j.addr.2020.12.016.
35. Mor, A., and Nicolas, P. (1994). The NH2-terminal alpha-helical domain 1-18 of dermaseptin is responsible for antimicrobial activity. J. Biol. Chem. *269*, 1934–1939.
36. Larrick, J.W., Hirata, M., Shimomoura, Y., Yoshida, M., Zheng, H., Zhong, J., and Wright, S.C. (1993). Antimicrobial activity of rabbit CAP18-derived peptides. Antimicrob. Agents Chemother. *37*, 2534–2539. https://doi.org/10.1128/AAC.37.12.2534.
37. Juba, M.L., Porter, D.K., Williams, E.H., Rodriguez, C.A., Barksdale, S.M., and Bishop, B.M. (2015). Helical cationic antimicrobial peptide length and its impact on membrane disruption. Biochim. Biophys. Acta *1848*, 1081–1091. https://doi.org/10.1016/j.bbamem.2015.01.007.
38. de Breij, A., Riool, M., Cordfunke, R.A., Malanovic, N., de Boer, L., Koning, R.I., Ravensbergen, E., Franken, M., van der Heijde, T., Boekema, B.K., et al. (2018). The antimicrobial peptide SAAP-148 combats drug-resistant bacteria and biofilms. Sci. Transl. Med. *10*, eaan4044. https://doi.org/10.1126/scitranslmed.aan4044.
39. Nell, M.J., Tjabringa, G.S., Wafelman, A.R., Verrijk, R., Hiemstra, P.S., Drijfhout, J.W., and Grote, J.J. (2006). Development of novel LL-37 derived antimicrobial peptides with LPS and LTA neutralizing and antimicrobial activities for therapeutic application. Peptides *27*, 649–660. https://doi.org/10.1016/j.peptides.2005.09.016.
40. Durr, U.H., Sudheendra, U.S., and Ramamoorthy, A. (2006). LL-37, the only human member of the cathelicidin family of antimicrobial peptides. Biochim. Biophys. Acta *1758*, 1408–1425. https://doi.org/10.1016/j.bbamem.2006.03.030.
41. Turner, J., Cho, Y., Dinh, N.N., Waring, A.J., and Lehrer, R.I. (1998). Activities of LL-37, a cathelin-associated antimicrobial peptide of human neutrophils. Antimicrob. Agents Chemother. *42*, 2206–2214. https://doi.org/10.1128/AAC.42.9.2206.
42. Li, X., Li, Y., Han, H., Miller, D.W., and Wang, G. (2006). Solution structures of human LL-37 fragments and NMR-based identification of a minimal membrane-targeting antimicrobial and anticancer region. J. Am. Chem. Soc. *128*, 5776–5785. https://doi.org/10.1021/ja0584875.
43. Büttner, K., Blondelle, S.E., Ostresh, J.M., and Houghten, R.A. (1992). Perturbation of peptide conformations induced in anisotropic environments. Biopolymers *32*, 575–583. https://doi.org/10.1002/bip.360320602.
44. Zhang, M., Ouyang, J., Fu, L., Xu, C., Ge, Y., Sun, S., Li, X., Lai, S., Ke, H., Yuan, B., et al. (2022). Hydrophobicity Determines the Bacterial Killing Rate of alpha-Helical Antimicrobial Peptides and Influences the Bacterial Resistance Development. J. Med. Chem. *65*, 14701–14720. https://doi.org/10.1021/acs.jmedchem.2c01238.
45. Drayton, M., Deisinger, J.P., Ludwig, K.C., Raheem, N., Müller, A., Schneider, T., and Straus, S.K. (2021). Host Defense Peptides: Dual Antimicrobial and Immunomodulatory Action. Int. J. Mol. Sci. *22*, 11172. https://doi.org/10.3390/ijms222011172.
46. Li, S.A., Xiang, Y., Wang, Y.J., Liu, J., Lee, W.H., and Zhang, Y. (2013). Naturally occurring antimicrobial peptide OH-CATH30 selectively regulates the innate immune response to protect against sepsis. J. Med. Chem. *56*, 9136–9145. https://doi.org/10.1021/jm401134n.
47. Bowdish, D.M.E., Davidson, D.J., Lau, Y.E., Lee, K., Scott, M.G., and Hancock, R.E.W. (2005). Impact of LL-37 on anti-infective immunity. J. Leukoc. Biol. *77*, 451–459. https://doi.org/10.1189/jlb.0704380.
48. Cai, Y., Wang, X., Zhang, T., Yan, A., Luo, L., Li, C., Tian, G., Wu, Z., Wang, X., Shen, D., et al. (2024). Rational Design of a Potent Antimicrobial Peptide Based on the Active Region of a Gecko Cathelicidin. ACS Infect. Dis. *10*, 951–960. https://doi.org/10.1021/acsinfecdis.3c00575.
49. Zhang, Z., Chen, Y., Gao, J., Yang, M., Zhang, D., Wang, L., Zhang, T., Cao, Q., Mwangi, J., He, C., et al. (2023). Orientational Nanoconjugation with Gold Endows Marked Antimicrobial Potential and Drugability of Ultrashort Dipeptides. Nano Lett. *23*, 11874–11883. https://doi.org/10.1021/acs.nanolett.3c03909.

STAR★METHODS

KEY RESOURCES TABLE

REAGENT or RESOURCE	SOURCE	IDENTIFIER
Bacterial and virus strains		
Escherichia coli	ATCC	ATCC 8739
Acinetobacter baumannii	ATCC	ATCC 19606
Pseudomonas aeruginosa	ATCC	ATCC 27853
Staphylococcus aureus	ATCC	ATCC 6538
Escherichia coli	Kunming Medical University	0894, 5017, 1007,1826, and 3401
Acinetobacter baumannii	Kunming Medical University	19110, 10769, 0357, 3228, and 4612
Pseudomonas aeruginosa	Kunming Medical University	90068, 60357, 52097, 17068, and 27450
Methicillin-Resistant *Staphylococcus aureus*	Kunming Medical University	Z, 11, 12, 21, 22, 41, 42, 51, and 52
Chemicals, peptides, and recombinant proteins		
TC-33	This study	N/A
TC-14	This study	N/A
SDS	Sigma	Cat#75746-250G
Luria-Bertani (LB) broth	OXOID	Cat#LP0021B
Dulbecco's modified Eagle's medium (DMEM)	CORNING	Cat#10013134
PBS	CORNING	Cat#21040086
Propidium Iodide (PI)	Solarbio	Cat#IP5030
RPMI1640 medium	CORNING	Cat#10040082
Vancomycin	MACKLIN	Cat#V871983
Colistin	Solarbio	Cat#P8350
Ampicillin	Solarbio	Cat#A6920
Critical commercial assays		
Cell Counting Kit-8	Med Chem Express	Cat#159077
Deposited data		
Reversed-phase high-performance liquid chromatography (RP-HPLC) and mass spectrometry	This study	Figure S2.
Experimental models: Cell lines		
Human HaCaT keratinocytes	ATCC	Cat# FS-0241
Software and algorithms		
ExPASy Bioinformatics Resource Portal	N/A	http://www.expasy.org/tools/
ChimeraX	N/A	https://www.cgl.ucsf.edu/chimerax/index.html
PyMOL	N/A	https://pymol.org/
PEP-FOLD3	N/A	http://bioserv.rpbs.univ-paris-diderot.fr/services/PEPFOLD3
GraphPad Prism 9.0	GraphPad Software	https://www.graphpad.com/

RESOURCE AVAILABILITY

Lead contact

Further information and requests for resources and reagents should be directed to and will be fulfilled by the lead contact, Zhiye Zhang (zhangzhiye5225@163.com).

Materials availability

All reagents generated in this study are available from the lead contact with a Materials transfer Agreement.

Data and code availability

- All data reported in this paper will be shared by the lead contact upon reasonable request.
- This paper does not report original code.
- Any additional information reported in this paper is available from the lead contact upon request.

EXPERIMENTAL MODEL AND STUDY PARTICIPANT DETAILS

Mouse model

All animal procedures were performed according to the standards described in the Guidelines for the Care and Use of Laboratory Animals of Institute of Medical Biology, Chinese Academy of Medical Sciences & Peking Union Medical College (DWSP202306005). All the experimental procedures using mouse blood samples were approved by the Research Ethics Board, Institute of Medical Biology, Chinese Academy of Medical Sciences & Peking Union Medical College.

METHOD DETAILS

Peptide synthesis

All peptides were synthesized by GL Biochem Ltd. (Shanghai, China) at purities exceeding 98%, as confirmed by reversed-phase high-performance liquid chromatography (RP-HPLC) and mass spectrometry.

Bioinformatic analysis and structural modeling

The physical and chemical parameters of the designed peptides were analyzed using the ExPASy Bioinformatics Resource Portal (http://www.expasy.org/tools/). The amphiphilicity of the peptides was analyzed using ChimeraX. The surface electrostatic potential of the peptides was analyzed using PyMOL. The helical wheel and secondary structures of the peptides were constructed using HeliQuest (http://heliquest.ipmc.cnrs.fr/) and PEP-FOLD3 (http://bioserv.rpbs.univ-paris-diderot.fr/services/PEPFOLD3), respectively.

Circular dichroism (CD) spectroscopy

The secondary structures of TC-14 were assessed by CD spectrometry (Chirascan V100, Applied Photophysics, UK) according to our previously described methods.[48] Briefly, TC-14 was first dissolved in either distilled water or sodium dodecyl sulfate (SDS) solution (0–64 mM) to a final concentration of 0.2 mg/mL. The CD spectra were recorded from 190 to 260 nm with a path length of 1 mm, step size of 1 nm, bandwidth of 1 nm, and time per point of 1 s at room temperature. The spectra of each sample represented the average of three scans after solution background subtraction.

Antibacterial properties *in vitro*

The minimal inhibitory concentrations (MICs) of the peptides against all bacterial strains were determined using a tube microdilution assay, as described in our previous study.[14] Four standard bacterial strains (*Escherichia coli* (*E. coli*) ATCC8739, *Acinetobacter baumannii* (*A. baumannii*) ATCC19606, *Pseudomonas aeruginosa* (*P. aeruginosa*)ATCC27853, and *Staphylococcus aureus* (*S. aureus*) ATCC6538) and 24 clinically isolated strains of *E. coli* (0894, 5017, 1007, 1826, and 3410), *A. baumannii* (19110, 10769, 0357, 3228, and 4612), *P. aeruginosa* (90068, 60357, 52097, 17068, and 27450), and methicillin-resistant *S. aureus* (MRSA) (Z, 11, 12, 21, 22, 41, 42, 51, and 52) were used in the assays. The bacterial strains were cultured in Luria-Bertani (LB) broth.

Cytotoxicity assay

In vitro cytotoxicity was assessed using a Cell Counting Kit-8 (CCK-8, Lot. No. 159077, Med Chem Express).[48] Human HaCaT keratinocytes (5×10^5 cells/well) were cultured in 96-well plates with Dulbecco's modified Eagle's medium (DMEM) for 24 h in a cell incubator (5% CO_2, 37°C). Peptide solutions (final concentrations of 3.125–100 μg/mL) were then added to the wells and incubated at 37°C for 24 h. The CCK-8 kit was then used according to the manufacturer's instructions. Thereafter, absorbance was measured at 490 nm using a microplate reader (Epoch, Bio Tek, USA). Each test was conducted in triplicate and repeated three times.

Hemolytic activity assay

To measure hemolytic activity, freshly obtained red blood cells from mice were washed several times in phosphate-buffered saline (PBS, pH 7.4), followed by centrifugation for 10 min and 1 200 × *g* at 4°C. The cells were then incubated at 37°C for 1 h in 0.9% saline with a series of peptide concentrations (1.563–100 μg/mL). Hemoglobin released in the supernatant was then measured at 540 nm with a microplate reader in accordance with previous study.[49]

Effects of plasma on TC-14 antibacterial activity

To determine the effects of plasma on the antibacterial activity of TC-14, the peptide (400 μg/mL) was incubated in saline solution with an equal volume of diluted mouse plasma at 37°C for 0, 0.5, 1, 2, 4, 6, and 8 h. The antibacterial activity of the peptide against *P. aeruginosa* ATCC27853, *A. baumannii* ATCC19606, and *S. aureus* ATCC6538 was evaluated at each time point based on MIC values.[48]

Bacterial membrane permeabilization assay

The impact of TC-14 on bacterial membrane permeabilization was determined using fluorescence assay according to our previously reported method.[48] In brief, the four bacterial strains were cultured in LB broth to the logarithmic growth phase, with the density of the bacterial solution then adjusted to 2×10^8 CFU/mL. Subsequently, 100 μL of bacterial suspension was added to a 96-well plate, followed by the addition of 10 μL of PI (2.5 μg/mL). Fluorescence measurements were taken for 15 min both before and after the addition of PI at an excitation wavelength of 535 nm and emission wavelength of 615 nm using a microplate reader (SynergyH1, BioTek, USA). Thereafter, 100 μL of TC-14 (1, 5, and 10 × MIC) or control (5 × MIC for colistin and vancomycin) was added, and changes in fluorescence were recorded for 60 min.

Scanning electron microscopy (SEM)

SEM was performed to study the possible mechanisms underlying TC-14 activity against bacteria. In brief, *P. aeruginosa* ATCC27853 and *S. aureus* ATCC6538 (approximately 2×10^8 CFU/mL) were incubated with TC-14 (5 × MIC) at 37°C for 30 min, followed by centrifugation for 10 min and 1000 rpm at 4°C. The resulting pellets were fixed with 2.5% buffered glutaraldehyde at 4°C for 2 h. The bacteria were then postfixed in 1% buffered osmium tetroxide for 2 h, dehydrated in a graded series of ethanol, frozen in liquid nitrogen-cooled tertbutyl alcohol, and vacuum dried overnight. After being mounting onto aluminum stubs and coated with gold via vacuum sputtering, the samples were analyzed using a Hitachi SEM (Regulus 8220, Hitachi, Japan) under standard operating conditions.

Transmission electron microscopy (TEM)

Exponential-phase bacteria (*S. aureus* ATCC6538 or *P. aeruginosa* ATCC27853) were treated with the peptide at 5 × MIC and 37°C for 30 min, then centrifuged for 10 min and 300 × *g* at 4°C. The resulting bacterial pellets were fixed with 2.5% buffered glutaraldehyde for 1 h, then postfixed with 1% buffered osmium tetroxide for 1 h, stained with 1% uranyl acetate, dehydrated in a graded series of ethanol, and finally embedded in white resin. Thin sections on copper grids were stained with 1% uranyl acetate and lead citrate. The buffer used was 0.1 M sodium cacodylate (pH 7.4). Microscopy was performed using a JEM microscope (JEM-1011, JEOL, Japan) under standard operating conditions.

Bacteria killing kinetics

In brief, *A. baumannii* ATCC19606 and *S. aureus* ATCC6538 were cultured in 1640 medium with 10% LB medium to the exponential phase (OD600 = 1.0), then diluted to 1×10^5 CFU/mL in 1640 medium with 10% LB medium and treated with peptide or control solutions (5 × MIC). Aliquots were taken at defined intervals and washed with 0.9% saline, then diluted appropriately in saline and plated on LB agar plates. The plates were incubated at 37°C for 24 h, and colony forming units (CFUs) were counted.

Drug-resistant assays

Bacterial passaging was conducted every 24 h based on our previous research.[48,49] In brief, bacteria were cultured on LB medium containing final MICs of 25%, 50%, 75%, 100%, 150%, and 200% for generations 1–10, 11–20, 21–30, 31–40, 41–50, and 51–60, respectively. After 60 consecutive generations, the bacteria were removed from the culture at five-generation intervals, and the MICs of the antimicrobial peptides against the above bacteria were examined.

Acute toxicity analysis

Female BALB/c mice (n = 6, 6–8 weeks old) were intravenously administered a single dose of TC-14 or control (colistin and vancomycin) at 10 mg/kg. After administration, mouse behaviors were monitored at different time points (10 min, 60 min, 12 h, 24 h, and 48 h). Toxicity was evaluated according to: normal fur and motility (without signs); ruffled fur and poor motility (mild signs); dyspnea, hutching, very ruffled fur, and complete immobility, even under stimulation (manifest signs).

Effects of TC-14 on mouse skin wound infections

The effects of TC-14 on mouse skin wound infections were determined according to our previous report.[48] In brief, female BALB/c mice (n = 6 or 7) were anesthetized, with their dorsal skin then shaved and disinfected with 70% ethanol. An incision was created on the dorsal surface with a 6-mm punch biopsy needle. At 4-h post-inoculation with 20 μL of *A. baumannii* (19606) and *S. aureus* (6538) (1×10^8 CFU/mL), a 20-μL dose of TC-14 (concentration range of 0.1 to 2 mg/mL) was applied to the wounded skin. Controls, including

saline (vehicle control), 0.5 mg/mL colistin, and 0.5 mg/mL vancomycin, were also administered. Bacterial colonization was quantified 2 h after these interventions.

QUANTIFICATION AND STATISTICAL ANALYSIS

Differences in mean values among different groups were assessed, expressed as mean ± standard deviation (SD). The Kolmogorov-Smirnov test was used for normal distribution analysis, followed by one-way analysis of variance (ANOVA) with *post hoc* Dunnett adjustment for *p* values. Data were analyzed using Prism v9.0 (GraphPad Software) and differences were considered significant at $p < 0.05$.